

Study of the fast ion confinement and current profile control on MAST

M. Turnyanskiy, D. L. Keeling, R. J. Akers, G. Cunningham, N. J. Conway, H. Meyer,
C. A. Michael, S. D. Pinches

EURATOM/UKAEA Fusion Association, Culham Science Centre, Abingdon, Oxon OX14
3DB, UK

e-mail contact of main author: mikhail.turnyanskiy@ukaea.org.uk

Abstract.

One of the main operational aims of the MAST experiment [1] and the proposed MAST upgrade is to investigate possible mechanisms to control the q-profile and drive off-axis current. Experiments were carried out to determine the extent to which the q-profile may be modified using two different approaches, transient and steady-state. Transient effects during the plasma current ramp-up phase were investigated with the aim of developing a start-up regime that can later be used as a target plasma for non-inductive current drive or to access advanced modes of operation such as the hybrid or improved H-mode. The most significant effect in this case was observed when early Neutral Beam Injection (NBI) was applied to the fast current ramp-rate start up plasmas causing reversed magnetic shear and the plasma current to ‘pile-up’ off-axis.

In steady-state experiments, in which off-axis NBI was studied, results indicate that broadening the fast ion deposition profile by off axis Neutral Beam (NB) injection helps to avoid harmful plasma instabilities and significantly extends the operational window of MAST. Long pulse ($>0.65\text{s}$) H-mode plasmas were achieved with plasma duration limited only by present machine and NBI engineering limits. In order to match the experimentally observed neutron rate and stored energy a low level of anomalous fast ion diffuse ion ($D_b \sim 0.5\text{m}^2\text{s}^{-1}$) is required. The introduction of the fast ion diffusion broadens the Neutral Beam Current Drive (NBCD) profile and degrades the relative contribution of NB driven current from $\sim 40\%$ to $\sim 30\%$. To obtain direct measurements of the current profile, a multi-chord Motional Stark Effect (MSE) diagnostic has been commissioned on MAST and is currently delivering first results in order to confirm the off axis location of the NB driven current.

1. Introduction

Determining the attractiveness of the Spherical Tokamak (ST) concept in the areas of high- β stability, confinement, non inductive current drive and divertor physics for pulse lengths

longer than the energy confinement time is a major mission of the MAST device. The high neoclassical resistivity observed in STs, and consequent faster current penetration rate, results in rapid approach to low values of core safety factor, q . This provides specific challenges for initiating $q_{\min} > 1$ regimes, desirable for long pulse or steady-state spherical devices. Determining the extent to which the q -profile may be modified during the plasma current ramp-up phase and developing a transient start-up regime is also a very valuable part of the present study. Such an approach may open a shortcut to achieve a desirable current profile much more rapidly by pre-shaping the initial q -profile that can later be used as a target plasma for non inductive current drive.

To achieve a steady state scenario in STs with $q_{\min} > 1$ both high efficiency current drive (CD) and current profile control is required which can potentially be provided by off axis NBCD. Driving current by an NBCD scheme is particularly important in STs due to the limited applicability of other non-inductive current drive schemes and because of the limited space available for neutron shielding of a solenoid. Optimisation of magnetic field alignment with NBI should be carefully considered as it has significant input on NBCD efficiency in STs. Finally, the understanding of fast ion physics in tokamak plasmas is important for the modelling, interpretation and extrapolation of off axis NBCD. Redistribution of the fast ions and degradation of the fast ion confinement caused by plasma instabilities is well known. For example, chirping “fishbone” modes have been seen to cause fast ion losses at rates up to 20% fast ion loss per burst in NSTX [2]. This would correspond to as much as a 50% reduction in fast ion population in steady state. Thus, understanding of the complex nature of interactions between the plasma instabilities and the beam ions and potential deviation from classical transport requires further investigation and is important for predictions of future larger tokamak facilities such as ITER [3].

2. Experiment and Diagnostics

MAST is a midsize low aspect ratio fusion research facility. The MAST plasma has a cross-section comparable to those of medium sized conventional tokamaks like ASDEX Upgrade and DIII-D, and has typical operational parameters of $R \sim 0.85\text{m}$, $a \sim 0.65\text{m}$, $I_p < 1.3\text{MA}$ and $B_t = 0.3\text{--}0.6\text{T}$. The heating system consists of two mid-plane co-injected deuterium neutral beams injected at a tangency radius, R_{tan} , of 0.7m . Experiments have benefited from the ongoing NBI upgrade to JET-style PINI sources allowing the studies to be extended to higher

power and duration (up to 3.9MW, 0.5s). By the end of the current upgrade, each injector will be capable of delivering 2.5MW of power extending the total NBI heating power to 5MW. The operational window of MAST has also been extended by the installation of error field correction coils, implementation of digital plasma control systems and a real time optical plasma edge detection and position control system. These improvements help to expand MAST operation space in low density plasmas and to control the current and the plasma shape during current ramp up and NBCD experiments. MAST is also well suited for these studies since it is equipped with a comprehensive set of modern plasma diagnostics and suitable modelling codes.

The electron density and temperature are measured using a 200Hz Thomson scattering (TS) diagnostic system and a single time 300 point system, ($\Delta r \sim 5\text{mm}$) [4]. The edge neutral density and edge density gradients are reconstructed from an absolutely calibrated linear D_α camera [5] [6] combined with local electron density and temperature from the MAST TS system. These diagnostics benefit from the distinctive MAST design feature, where the outboard edge and tokamak vessel are separated by a significant distance, providing viewing beyond the plasma edge [7]. The performance of the beams is monitored by beam emission imaging spectroscopy [8] delivering time resolved measurements of the beam fast neutral density and reinforcing data on the NBI geometry for beam modelling codes. A 2D visible bremsstrahlung imaging camera [9] which provides Z_{eff} profiles using TS data, and an infra red camera for diagnosing power flow to the diverter targets and particle loss to in-vessel components [10] are also available. Recently, the first direct measurements of the current profile by a 20-chord (35 planned) Motional Stark Effect (MSE) [11] diagnostic have become available. The MSE diagnostic has spatial resolution $\Delta r \leq 2.5\text{ cm}$, temporal resolution $\Delta t \leq 5\text{ ms}$ and is capable of measuring the polarisation angle with $\Delta\alpha \leq 0.5^\circ$ accuracy and will provide a test of current drive and transport theory and modelling. Future plans include direct incorporation of the MSE data as input into the transport modelling.

The Larmor orbit corrected Monte Carlo TRANSP code [12] is routinely used on MAST to model transport, heating and current drive. The code simulations incorporate the measured profiles of T_e , n_e and T_i inside the separatrix from TS measurements and Charge eXchange Recombination Spectroscopy (CXRS), T_e , n_e in the scrape-off layer (SOL) from Langmuir probe measurements and the neutral particle fluxes from the D_α camera. Equilibrium reconstruction derived from EFIT [13] and experimentally measured Z_{eff} profiles are also incorporated.

3. Current ramp phase

In order to investigate the extent to which the q -profile may be modified during the current ramp-up phase a test set of MAST plasma discharges has been established. Three different parameters were investigated separately: the current and density ramp rates and the NBI start-time. Two rates of current ramp, fast (7MA/s) and slow (3.5MA/s) were used in combination with fast ($8.8 \times 10^{20}/\text{m}^3.\text{s}$) and slow ($4.9 \times 10^{20}/\text{m}^3.\text{s}$) density ramps. In all beam heated discharges, NBI (1.4MW, 45keV) was applied at four different stages of the current ramp, corresponding to the beginning, third, two thirds and the end of the current ramp. Other plasma parameters such as shape of the plasma boundary, position and current value at the flat-top were kept constant. The TRANSP code was used to model the current penetration in these experiments [14]. The code interpretive analysis uses experimentally obtained plasma profiles and solves the Poloidal Field Diffusion Equation (PFDE) self-consistently with the neoclassical resistivity and calculated non-inductive current drive. The analysis was started at the earliest time an acceptable EFIT equilibrium could be produced. An EFIT equilibrium reconstruction, constrained only by external magnetic measurements, was used to provide the time dependent plasma boundary and the initial q -profile for TRANSP. The simulation setup was adjusted so as to achieve the best match possible to the available MHD data. The main change in the setup involved varying the time at which the evolution of the q -profile is changed from an interpretive analysis of EFIT to evolving the q -profile using the PFDE, effectively changing the initial estimate of the q -profile shape which is supplied to the PFDE. It was found that choosing initial conditions such that the q -profile evolution matches the time and q_{\min} value of the first Alfvén cascade, reproduced the expected reversed magnetic shear, and the arrival time of the $q=1$ surface in the TRANSP simulation was sufficiently close to the appearance of the sawtooth precursor mode as determined from soft X-ray data. It is noted that there was no need to invoke any anomalous resistivity [14] to achieve this match.

Results and discussions

The q -profiles for each discharge were examined at the start of the current flat-top (200ms for the slow current ramp experiments, 105ms for the fast current ramp experiments) and are shown in Figure 1a. All simulations performed for NB heated plasmas show negative values

of magnetic shear, $s = \left(\frac{r}{q} \right) \left(\frac{dq}{dr} \right)$ (i.e. reversed magnetic shear), a necessary condition for the observed Alfvén cascades. Early NBI was most effective with the most pronounced effect being seen with the fast current ramp-rate. In these scenarios a strong reversed magnetic shear developed with the addition of early beams with q_{\min} positioned at $0.3 < r/a < 0.55$ as illustrated in Figure 1a. In Ohmic discharges, neither current nor density ramp rate had a very strong effect on the core of the MAST plasma. However, in the outer half of the plasma, $0.5 < r/a < 1$, magnetic shear moderately increases for the faster density and decreases for the faster current ramp rates as shown in Figure 1b.

The generation of negative magnetic shear by on-axis beams is explained by the TRANSP modelling. The changes in the q -profile shown in Figure 1a are due to changes in the Ohmic current profile rather than the presence of beam driven current which is peaked close to the plasma axis ($r/a=0.15-0.2$) and, in these discharges, accounts for only 5-7% of the total plasma current, I_p . In contrast the Ohmic current contribution by the end of the ramp up phase (~ 120 ms, in $8.8 \times 10^{20}/\text{m}^3 \cdot \text{s}$ fast current ramp discharges) accounts for around 90% of total I_p and peaks off-axis ($r/a=0.4-0.5$). Simulations show that the on axis NB heats the core and peaks the electron temperature profile consequently lowering core plasma resistivity and the current diffusion rate and causing the current to ‘pile-up’ off-axis. Increased off-axis current density results in reversed magnetic shear. Examination of later times in the TRANSP runs shows that this is a dynamic effect and the plasma relaxes to a state with a monotonic q profile as the Ohmic current slowly penetrates into the core. The temperature dependence of the current penetration rate also explains the increased magnetic shear in the fast density-ramp Ohmic discharges where a flatter density profile is obtained compared to the slower density ramp-rate discharges. The total plasma pressure, and the central values of n_e and T_e were similar in presented Ohmic experiments so the less peaked density profile results in a more peaked temperature profile affecting the Ohmic current penetration rate. The outer half of the plasma is mainly affected since the current profile has not had sufficient time to relax and penetrate to the centre; the resulting differences in magnetic shear can be seen in Figure 1b. On the other hand the flatter density profile also affects the neutral beam deposition and resultant beam-driven current profiles giving similar magnetic shear in all the early beam heated discharges. Despite being a transitory effect, a combination of the described technique with off axis current drive schemes represents a powerful tool for generating the necessary q -profiles for steady state plasmas.

3. Off axis NBI on MAST

One of the most promising approaches for broadening and shaping the plasma current profile in tokamaks is off axis NB injection. At present, the MAST NBI systems can not be reoriented to study off axis NBCD in DND (Double Null Divertor) plasmas. However, the flexibility offered by the large MAST vessel has been exploited for the study of off axis heating in vertically displaced SND (Single Null Divertor) plasmas. Plasma configurations with beam tangency radius of about half the minor plasma radius have been achieved in SND discharges by displacing the MAST plasma by up to 0.3m in the vertical direction as shown in Figure 2 for the lower SND plasma configuration. The tangency point of NBI is highlighted as a cross at $R=0.7\text{m}$, $Z=0\text{m}$. Recent improvement in optimization of the plasma formation allowed an increase of the plasma volume in MAST SND scenarios, reaching up to 90% of the volume of a typical MAST DND discharge.

Magnetic field alignment with NBI on MAST

The MAST tokamak is an up-down symmetric machine where Ohmic, inductively driven, lower and upper SND discharges are nearly identical [15]. They also exhibit a similar low level of impurity accumulation and tend to have very similar heating properties. The extreme geometry of low aspect ratio devices, however, can have a strong effect on the NBCD efficiency in SND discharges due to the well known classical effect of magnetic field alignment with the direction of NBI. For example, the effects of NBI alignment with the plasma magnetic field on fast ion confinement can be validated by changing the direction of the toroidal field, B_T . Similar results can also be achieved by comparing plasma performance using upper SND and lower SND configurations. Fast ions born above the mid-plane (lower SND) have a significantly different birth pitch-angle distribution to those born below the mid-plane (upper SND) due to the opposite direction of the radial component of the poloidal field at the location of predominant NB deposition. This effect is much enhanced in STs due to the relatively large ratio of poloidal to toroidal field. In conventional tokamaks the toroidal field greatly exceeds the poloidal magnetic field so the effect on NBCD should be less pronounced. The described effect provides a means of testing the location of NB driven current and model

predictions. In the MAST, preferential beam-field alignment, when a higher proportion of the fast particles is deposited on better confined passing orbits, is obtained if the beam is injected above (lower SND configuration) rather than below (upper SND configuration) the magnetic axis. For example, the higher efficiencies of off axis current drive in lower SND plasmas in MAST should keep the current profile broader for longer, delaying the appearance of the $q=1$ surface in two otherwise identical lower and upper SND discharges. Soft X-Ray (SXR) measurements, Thomson scattering measurements and data from the EFIT equilibrium reconstruction code are compared in Figure 3 for beam injection into similar upper SND and lower SND target plasmas. All test discharges have $I_p \sim 620 \text{ kA}$, $\bar{n}_e \sim 3 \cdot 10^{19} \text{ m}^{-3}$, $T_e \sim 1 \text{ keV}$, $P_{\text{NBI}} \sim 1.7 \text{ MW}$ and the same up-down mirrored plasma boundary. Estimates of the time of $q=1$ appearance and I_i from EFIT are presented with lower plasma inductance and a delay in $q=1$ appearance being observed in lower SND plasmas relative to upper SND and Ohmic discharges, indicative of greater off axis NBCD in lower SND, as predicted from simulations. To avoid potential distortion of the results by transient events such as ELMs, the data was compared during the L-mode phase of the discharge. Modelling by TRANSP shows that in the case of unfavourable NBI alignment (upper SND) and in line with results recently reported on other tokamak experiments [16], the NBCD efficiency is almost halved. Due to such significant degradation in NBCD performance in upper SND, our main off axis NBI studies as well as further results presented in this paper have concentrated on the case of the lower SND plasma configuration, where NB is injected above the plasma mid-plane i.e. along the plasma magnetic field lines.

Plasma performance with off axis NBI

The future generation of STs relies heavily on off axis NBI power for both, generating and controlling the current profile and for efficient plasma heating [17][18]. The fast ion confinement with off axis NBI is a particular concern for spherical tokamaks with their low toroidal magnetic field and its strong variation between the inboard and outboard plasma edge. As a result, energetic ion orbit topologies differ significantly from similarly sized conventional tokamaks [19]. The Larmor radius is comparable to the radial extent of the drift orbit with the gyromotion a significant perturbation relative to the guiding centre trajectory. Typically, 40 keV co-injected trapped deuterium ions in MAST can have a poloidal projection of the gyroradius of $\rho_L \sim 25 \text{ cm}$, similar in magnitude to the banana orbit width and

more than one third of the typical MAST plasma minor radius ($a \sim 65\text{cm}$) raising a potential concern for the classical losses of the fast particles especially during off axis NBI.

Examples of typical distributions of co-passing fast ions ($V_{\parallel}/V \sim 0.7-1$), simulated by TRANSP code under an assumption of classical beam deposition and collisional thermalisation with on and off axis NBI are shown in Figure 2. The energy range of the fast ion distribution here expands to the end of the high energy tail of the Maxwellian distribution with the lower cut-off energy is at $3T_i$. The effect of the off axis NB deposition is clearly visible and results in much wider deposition of the passing fast ions. Experimental results indicate that broadening the fast ion deposition profile by off axis NB injection helps to avoid harmful plasma instabilities such as sawtooth driven disruptions and significantly extends the operational window of MAST. Long pulse plasmas ($>0.65\text{s}$) with a long H-mode duration were achieved and were limited only by present machine and NBI engineering limits. These off axis heated plasmas have shown high plasma performance with high sustained β_N ($\sim 3.5-4$). Efficient off axis NBI heating has been experimentally confirmed by the behaviour of plasma parameters such as plasma energy, ion and electron temperature and neutron yield. Comparison of the electron temperature and density profiles in Ohmic (black diamonds) and off axis heated lower SND plasmas (red triangles) is shown in Figure 4. The ion temperature profile (blue squares) is also shown for the NBI heated case. Both electron and ion temperatures increase significantly from $\sim 0.5\text{keV}$ to $\sim 1.5\text{keV}$. The recent introduction of digital plasma density feedback control allowed beam heated and Ohmic discharges to be controlled with very similar density profiles which are also presented in Figure 4. Experiments to date demonstrate comparable plasma heating for off axis heated discharges (strongly SND) to that achieved with on axis heated discharges with similar plasma current and electron density. Electron temperature, neutron yield and plasma stored energy in on- and off-axis heated NBI discharges ($I_p \sim 600-650\text{kA}$, $P_{\text{NBI}} \sim 3-3.5\text{MW}$, beam energy $E_b = 60\text{keV}$) are shown in Figure 5. Red triangles and black circles represent the flattop average and discharge maximum values respectively. Strongly off axis SND discharges pose a challenge for detailed transport analysis on MAST, due to the majority of diagnostic measurements being located in the vessel rather than plasma mid-plane (see Figure 2). Some data extrapolation into the region with $0 < \psi < 0.15$ is unavoidable. The central region of MAST plasma ($0 < \psi < 0.15$) usually exhibits flat T_e , n_e and Z_{eff} profiles limiting possible uncertainties in the missing diagnostic data to 10-15%. Sensitivity studies, where missing diagnostic data was varied within realistic upper and lower limits, produced robust results, insensitive to such

variations, and resulted in an uncertainty in simulated NBCD current of less than a few % at most. Modelling assumptions for diagnostic measurements used in SND simulations were further validated by shifting the SND plasma back to the vessel midplane (to optimise diagnostic measurements) in a time scale much faster ($<1\text{ms}$) than both MAST confinement and beam ion slowing down times.

Efficient generation of off axis plasma current by NBCD and the bootstrap effect in MAST are also predicted by theory [3] but determining the exact non-inductive contribution is currently a challenging task due to the large Ohmic fraction of the plasma current. TRANSP simulations indicate that with present NBI power (up to $\sim 3.9\text{ MW}$, $E_b=60\text{keV}$) MAST plasmas have an NB driven current contribution of up to $\sim 40\%$. Plasma discharges with $P_{\text{NBI}} < 2\text{ MW}$ on MAST are usually free of fast particle driven MHD and TRANSP modelling, assuming classical beam deposition and using Chang-Hinton model [19][20] agrees well with the experimentally measured plasma parameters such as the total neutron yield, the plasma stored energy and loop voltage and the neutral particle fluxes detected by the scanning Neutral Particle Analyser (NPA) [21][22]. The behaviour of the fast ions in such moderate NBI powered discharges in both MAST L- and H-mode plasmas has been investigated and reported in [22]. The agreement of the modelling with experiment indicates that the beam ion population in the co-injected MAST plasmas studied ($P_{\text{NBI}} < 2\text{ MW}$) evolves predominately due to Coulomb collisions and charge exchange phenomena and confirms the classical behaviour of the fast ions. The fast ion losses were low (a few %) and dominated by charge exchange. There was no strong evidence of any anomalous slowing down, for example due to fast particle MHD interactions. This conclusion is also qualitatively supported by the observed quiescence of the plasma discharges studied *i.e.* no fast particle driven MHD activity observed.

However, in initial experiments with $P_{\text{NBI}} > 3\text{MW}$ both the experimentally measured stored plasma energy and volume average neutron rate are significantly lower than the values calculated by TRANSP assuming classical beam ion thermalisation. A spectrogram (Figure 6) from a mid plane magnetic coil shows extensive fish-bone activity between 10 and 30 kHz during high power NBI (MAST#18808). Both experimentally measured and TRANSP simulated neutron rates are also presented. The measured neutron flux is a good monitor of the fast ion behaviour in MAST as it is dominated by the beam-plasma reactions. Due to the large energy difference between the energy of the beam ($\sim 60\text{keV}$) and the plasma ions ($T_i \sim 1\text{--}1.5\text{keV}$), the cross-section for D-D fusion is higher for such beam-plasma reactions than for

the thermal plasma-plasma reactions. The time of the largest discrepancy between simulated and measured neutron rates (0.2s-0.35s) correlates well with the highest magnitude of observed $n=1$ fishbone magnetic activity suggesting appreciable anomalous beam-ion radial transport associated with this beam driven MHD. The degradation of the beam-ion confinement is analysed in more detail in Figure 7. The TRANSP code permits introduction of an *ad hoc*, pitch angle independent, beam-ion diffusion coefficient, D_b . The code also has the capability of varying the magnitude of this non-classical, anomalous fast ion diffusion as a function of time, space and energy of the fast particles involved. Comparison with the experimentally measured neutron rate indicates that a diffusion coefficient of roughly $D_b = 0.5\text{-}1\text{ m}^2\text{s}^{-1}$ is required to account for the measured rate, comparable to that previously reported from DIII-D [23], AUG [24], JET [25] and NSTX [26]. An assumed level ($D_b = 0.5\text{-}1\text{ m}^2\text{s}^{-1}$) of the fast ion diffusion also improves the agreement with the stored energy measurements and provides a useful check on this hypothesis. The introduction of anomalous fast ion diffusion only during the observed $n=1$ fishbone magnetic activity (0.2s-0.35s), and for fast ions with energy above 40keV, proved to be sufficient to match the experimentally measured stored energy and neutron rate with TRANSP simulations. Other plasma parameters with large systematic uncertainties such as neutral density, edge ion temperature and, for the discharge studied here, toroidal velocity affecting fast ion confinement were varied within realistic upper and lower limits. The simulated neutron rate and stored energy have proven to be very robust to those variations. For example, increasing the neutral density by a factor of ten led to only a very modest (2-3%) drop in simulated neutron rate and stored energy. The calculated fractions of the total plasma current, I_p , distributed between Ohmic, bootstrap and neutral beam driven components for $D_b = 0.5\text{ m}^2\text{s}^{-1}$ are shown in Figure 7 together with TRANSP simulations and experimental measurements of various other plasma parameters. Although this analysis is useful as an indication of the magnitude of the anomalous beam ion transport, this simplistic *ad hoc* model can not accurately predict the actual beam ion profile, which depends on details of the resonant interaction between the instabilities and the beam ions. Work is ongoing, using the HAGIS δf MHD model [27], to introduce spatially limited, energy and pitch angle dependent beam-ion diffusion which can describe the resonant nature of the interaction between the plasma instabilities and the beam ions in more detail.

NB driven current is mainly generated by the fast ions located on co passing orbits. The density of the fast ions and spatial distribution of such orbits are directly correlated with the amount of NB generated current and its location. TRANSP simulated poloidal projections of

co-passing fast ion distributions with $V_{||}/V \sim 0.7-1$ with ($D_b = 1 \text{ m}^2\text{s}^{-1}$) and without ($D_b = 0 \text{ m}^2\text{s}^{-1}$) anomalous fast ion diffusion are shown in Figure 8. The degrading effect on the fast ion confinement, caused by anomalous fast ion diffusion, is clearly visible and results in both a decrease in the fast ion density and a smearing of the off axis location of the co passing fast ions. As a result, the NB driven radial current profile broadens and its relative contribution to the total current is decreased. Corresponding TRANSP simulations of NB driven current density profiles for various values of D_b are shown in Figure 9. Modelling results show that for the inferred values of $D_b = 0.5-1 \text{ m}^2\text{s}^{-1}$, the NBCD contribution is typically decreased from $\sim 40\%$ to $\sim 30\%$ of the total plasma current. The calculated neutral beam driven current and its relative contribution to the total current for various values of D_b are summarized in Table 1. Despite the predicted degradation of NB driven current caused by anomalous fast ion diffusion, the predicted NBCD current amounts to $\sim 200\text{kA}$ and remains a substantial non-inductive contribution to the total I_p in this 600kA discharge. The remarkable resilience of the MAST off axis NBI discharges to sawtooth driven disruptions requires further investigation. Besides current profile broadening by NBCD, other effects such as fast ion sawtooth destabilisation by off axis NBI [28] may play a role.

$D_b \text{ (m}^2\text{s}^{-1}\text{)}$	0	0.3	0.5	1.0	2.0
$I_{\text{NBCD}}(\text{kA})$	253	221	209	164	130
$I_{\text{NBCD}}/I_p (\%)$	41	36	34	27	21

Table 1. Maximum NB generated current (at $t=0.22\text{s}$) and its relative contribution to the total current calculated by TRANSP for various values of anomalous fast ion diffusion coefficient, D_b . D_b is pitch angle independent and is only applied during the observed $n=1$ fishbone magnetic activity ($0.2\text{s}-0.35\text{s}$) and for fast ions with energy above 40keV .

4. First MSE results

Direct measurements of the current profile are highly desirable and a multi-chord MSE diagnostic [11] is being developed to confirm the off axis location of the NBI driven current. First multi-chord MSE data have recently been obtained on MAST. As the MSE diagnostic commissioning coincided with ongoing NBI upgrades on MAST only one NBI line with

limited beam power (up to 1.85MW) was available, limiting the diagnostic performance and availability and affecting the high accuracy required for the TRANSP analysis of these discharges. Nevertheless the first results are encouraging. Polarisation angles in off axis NBI discharges together with the resulting current density distributions for a set of MAST discharges with identical plasma current and boundary are shown in Figure 10. Three plasma discharges are presented; Ohmic reference shot with line average electron density $\sim 2 \cdot 10^{19} \text{ m}^{-3}$ and two NBI heated discharges, where 1.85MW of NB power was injected, with line average electron densities $\sim 2 \cdot 10^{19} \text{ m}^{-3}$ and $4 \cdot 10^{19} \text{ m}^{-3}$ respectively. Ohmic MSE data has been obtained by short pulsing the MAST heating beam at the time of interest (0.2s) i.e. using the MAST NBI as a non-perturbative diagnostic tool and preserving the Ohmic plasma properties. As NB driven current is predicted to diminish rapidly with increased plasma density, one of the test discharges was repeated with line average electron density doubled from $2 \cdot 10^{19} \text{ m}^{-3}$ to $4 \cdot 10^{19} \text{ m}^{-3}$ in order to minimise the amount of beam driven current. To minimise the influence of $n=1$ MHD instabilities such as sawteeth, the data shown in Figure 10 were obtained just before appearance of the $q=1$ surface but after sufficient time for any effects caused by the current ramp up to have become negligible. Despite the limited NBI power available (1.85MW), clear differences in polarisation angle are observed in the three cases. The measured current profiles are consistent with significant off axis NBCD at low density, diminishing as the density is increased. The measurements also reproduce the Shafranov shift due to NBI heating. All presented analysis was performed using EFIT95 with a simple 1D MSE constraint. Full generalised MSE constrained EFIT++ which will include full beam and MSE optics is currently under development.

5. Conclusions

The generation of negative magnetic shear by on axis beams is explained by the TRANSP modelling. Simulations confirm quantitatively that the peaking electron temperature profile lowers core plasma resistivity and the current diffusion rate and causes the current to ‘pile-up’ off-axis to an extent consistent with observations. MHD signatures were used to benchmark the TRANSP modelling. For example, the value of q_{\min} during the appearance of Alfvén cascades led to an accurate prediction of the time of the first sawtooth without invoking any anomalous resistivity. Despite being a transitory effect, the presented technique of early core heating to slow current penetration represents a powerful tool for controlling and

shaping the q-profile on MAST. This technique combined with off axis NB, as envisaged for the proposed upgrade to MAST, will allow rapid formation of a steady-state compatible q-profile and maintenance of this profile to demonstrate potential steady-state operation.

Off axis NBI experiments on MAST benefited from the ongoing NBI upgrade and demonstrate plasma heating and neutron yield for off axis heated discharges (strongly SND) comparable to that achieved with on axis heated discharges with similar plasma current and electron density. Low NBI power discharges ($P_{\text{NBI}} < 2 \text{ MW}$) on MAST are typically free from fast particle driven MHD and TRANSP modelling based on classical beam physics agrees well with the experimental measurements. Introduction of high power off axis NBI (up 3.9MW) led to appearance of n=1 fishbone magnetic activity in these initial experiments. Comparison of experimentally measured volume averaged neutron rate and stored plasma energy with the rates calculated by the TRANSP code, using an assumption of classical beam deposition and collisional thermalisation in these discharges, shows that the experimental values are significantly overestimated (by ~25-30%). The time of the largest discrepancy between simulated and experimental data correlates well with the highest magnitude of observed n=1 fishbone magnetic activity suggesting appreciable anomalous beam-ion radial transport associated with this beam driven MHD. A level of anomalous fast ion diffusion with diffusion coefficient of roughly $D_b = 0.5\text{-}1\text{m}^2\text{s}^{-1}$ is needed to account for the experimental measurements degrading the relative contribution of NB driven current from ~40% to ~30% of the total plasma current. Nevertheless the TRANSP simulations suggest that, despite some decrease in NB generated current and broadening of the NBCD profile, the driven current remains off axis consistent with the first data from the new multi-chord MSE diagnostic which has recently been commissioned on MAST.

Extensive transport simulations show that a combination of efficient non-inductive current drive and heating is possible in larger scale spherical devices such as MAST-U providing encouraging prospects for the use of off axis NB injection in future plasma devices.

This work was funded jointly by the United Kingdom Engineering and Physical Sciences Research Council and by the European Communities under the contract of Association between EURATOM and UKAEA. The views and opinions expressed herein do not necessarily reflect those of the European Commission

Reference

1. Darke A. C. et al, Proc. of the 18th Symposium on Fusion Technology, Karlsruhe, Germany, 799, (1994)
2. Fredrickson E. D. et al, Phys. Plasmas 10 2852 (2003)
3. ITER Physics Basis Editors 1999 Nucl. Fusion 39 2175
4. Walsh M. J. et al, Rev. Sci. Instrum. 74 1663 (2003)
5. Tournianski M. R. et al, Nucl. Fusion 41 77 (2001)
6. Tournianski M. R. et al, Rev. Sci. Instrum. 74 2089 (2003)
7. Carolan P. G. et al, Rev. Sci. Instrum. 75 4069 (2004)
8. Patel A. et al, Rev. Sci. Instrum. 75 4145 (2004)
9. Patel A. et al, Rev. Sci. Instrum. 75 4944 (2004)
10. Lott F. et al, Journal Nucl. Materials, 337-339, 786 (2005)
11. De Bock M. F. et al, Rev. Sci. Instrum. 79 10F524 (2008)
12. Goldstone R. J. et al, J. Comput. Phys. 43 61 (1981)
13. Lao L. L. et al 1985 Nucl. Fusion 25 1611
14. Keeling D. L. et al, Proc. of 35th EPS Plasma.Phys.Conf., Greece (2008), P-1.073
15. Tournianski M. R. et al, Proc. of 33th EPS Plasma.Phys.Conf., Rome (2006), P-1.099
16. Murakami M, Proc. “Off-Axis Neutral Beam Current Drive for Advanced Scenario Development in DIII-D”, submitted to Nucl. Fusion (2009)
17. Wilson H. R. et al, Nucl. Fusion 44 917 (2004)
18. Akers R. J. et al, Nucl. Fusion 40 1223 (2000)
19. Chang C.S., Hinton F. L., Phys. Fluids 25 1493 (1982)
20. Chang C.S., Hinton F. L., Phys. Fluids 29 3314 (1986)
21. Akers R. J. et al, Plasma Phys. Control. Fusion 45 A175 (2003)
22. Tournianski M. R. et al, Plasma Phys. Control. Fusion 47 671 (2005)
23. Heidbrink W. W. et al, Nuclear Fusion 42 972 (2002)
24. Gunter S. et al, Nuclear Fusion S98 45 (2005)
25. Baranov Yu. F et al, Plasma Phys. Control. Fusion 51 044004 (22pp) (2009)
26. Menard J. E. et al, Nucl. Fusion 47 (2007) S645
27. Pinches S. D. et al, Comp.Phys.Comm., 111, 1,133-149 (17), (1998)
28. Chapman I. T. et al, Nuclear Fusion 49 035006 (2009)

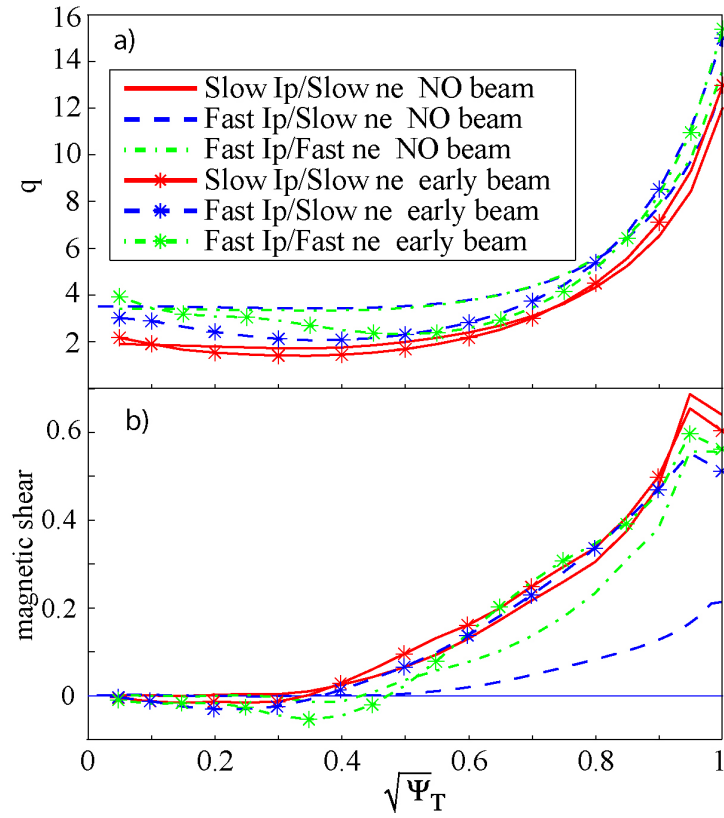


Figure 1. Comparison of q and magnetic shear profiles at the end of the current ramp from experiments with no NBI and with NBI starting 35ms (70ms for slow I_p ramp case) i.e. at the time when $I_p = 1/3 I_p(\text{flat-top})$.

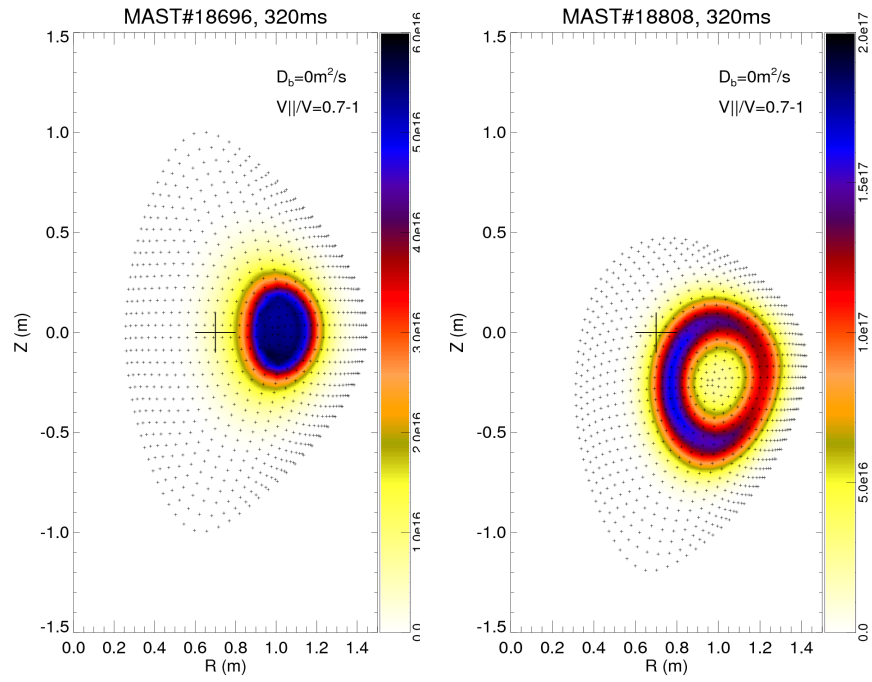


Figure 2. TRANSP simulated poloidal projections of co passing fast ion distributions with $V_{||}/V \sim 0.7-1$ under an assumption of classical beam deposition and collisional thermalisation with on (left) and off (right) axis NBI. The tangency point of NBI is

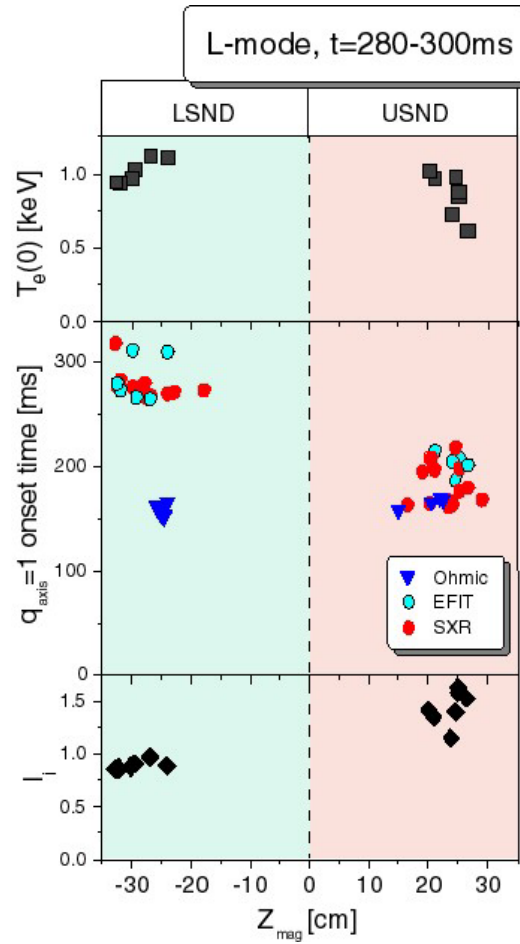


Figure 3. central electron temperature T_e , $q_{\text{axis}}=1$ onset time and internal inductance I_i for a test set of similar upper and lower SND plasma discharges are compared versus the vertical shift of the MAST magnetic axis relative to the mid-plane. The estimates of the time of $q=1$ appearance and I_i from EFIT code are also presented.

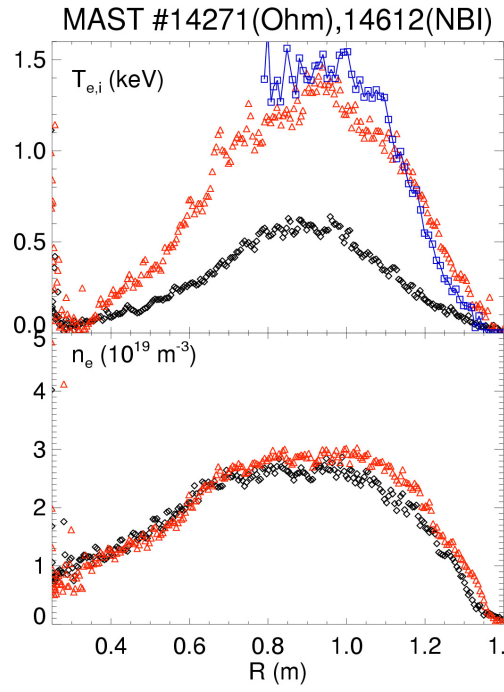


Figure 4. Comparison of the electron temperature and density profiles in Ohmic (black diamonds) and off axis NBI heated SND plasmas (red triangles), $P_{\text{NBI}}=1.7\text{MW}$, $B_t=0.55\text{T}$, $I_p=620\text{kA}$. The ion temperature profile (blue squares) is also presented for the NBI heated case.

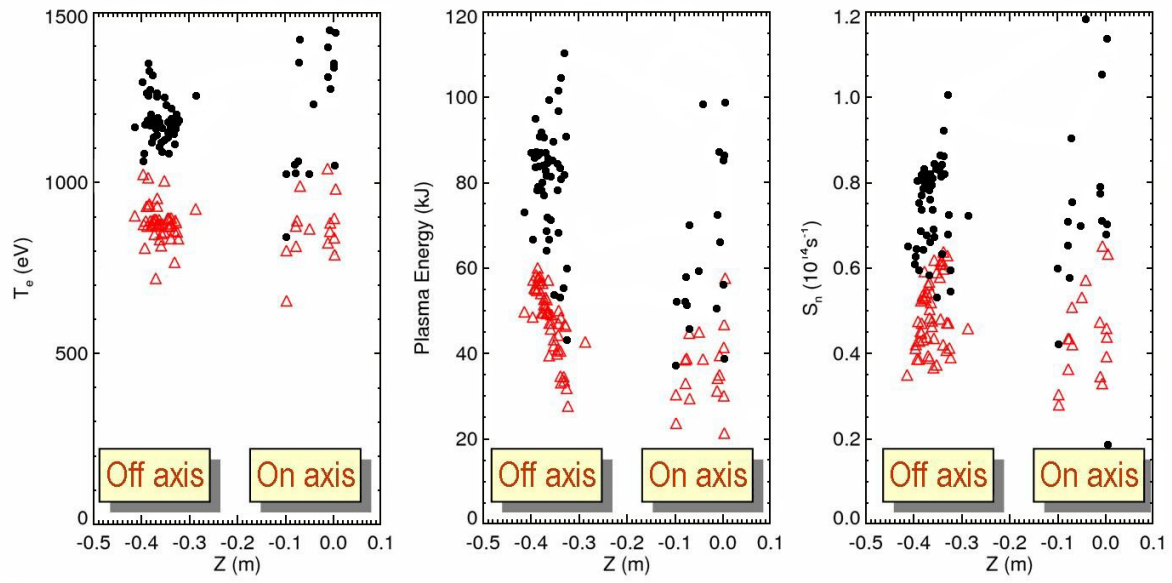


Figure 5. Central electron temperature, stored energy and neutron yield in on ($|Z| \sim 0$ cm) and off ($|Z| > 0.3$ m) axis NBI discharges. Red triangles and black circles are the flattop average and discharge maximum values respectively.

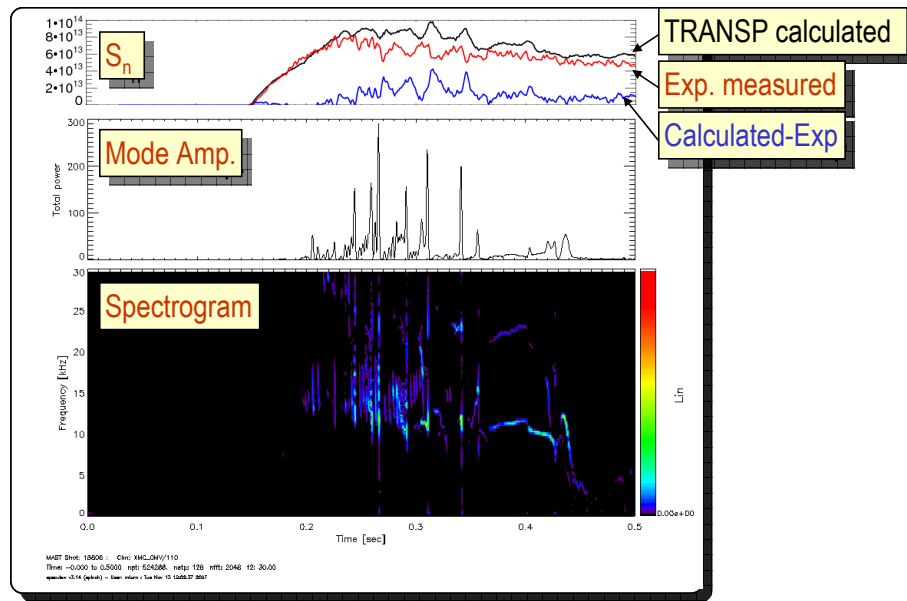


Figure 6. A spectrogram from a mid plane magnetic coil shows extensive fish-bone activity between 10 and 30 kHz during high power NBI (MAST#18808). Time of the largest discrepancy between simulated and measured neutron rates (0.2s-0.35s) correlates well with the magnitude of the observed MHD suggesting appreciable MHD driven anomalous beam-ion radial transport.

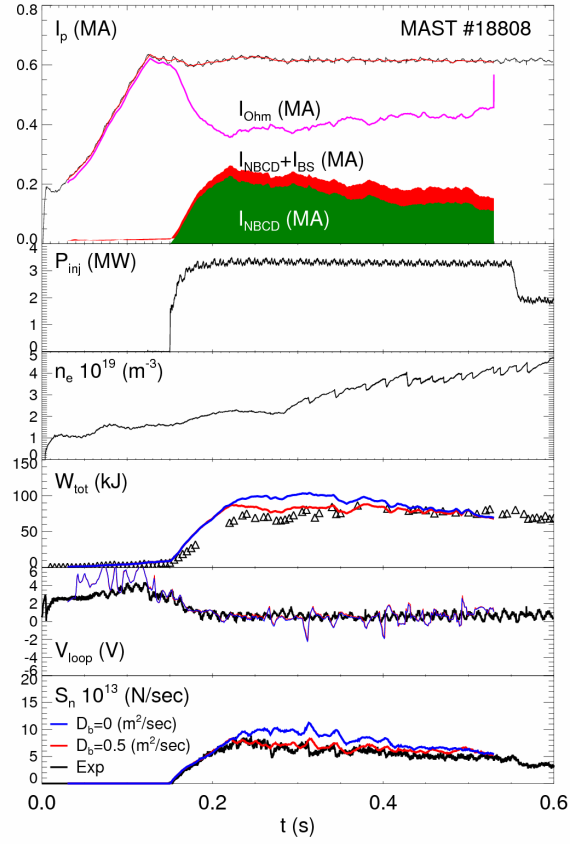


Figure 7. TRANSP simulated distribution of the total plasma current, I_p , between Ohmic, the bootstrap and neutral beam driven components for $D_b = 0.5 \text{ m}^2\text{s}^{-1}$. Experimentally observed neutron yield, edge loop voltage and stored energy are compared with TRANSP simulations for $D_b = 0$ and $0.5 \text{ m}^2\text{s}^{-1}$. Time history of the total injected NBI power, line average electron density are also shown.

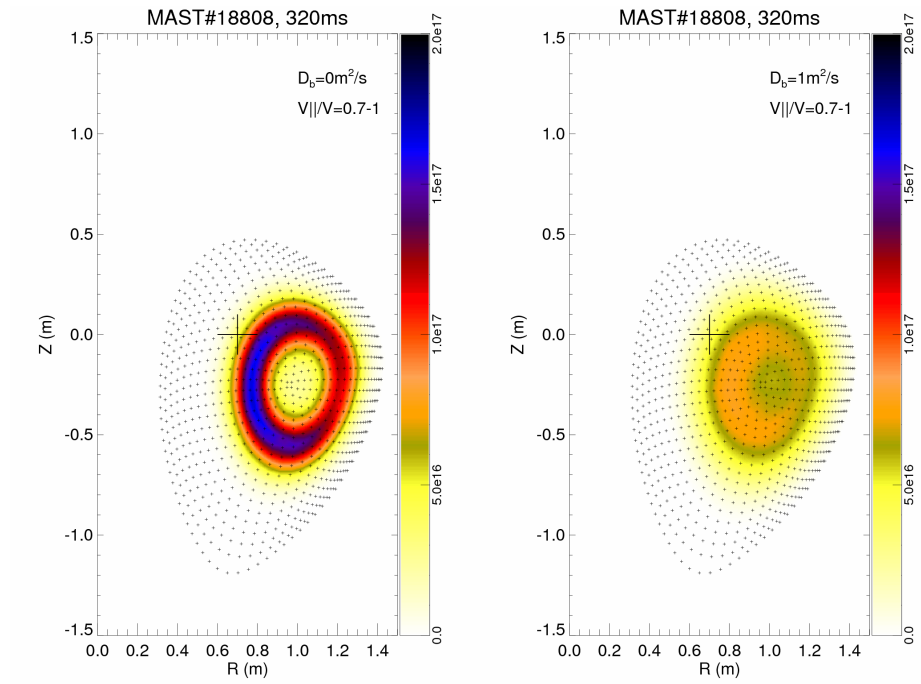


Figure 8. TRANSP simulated poloidal projections of co passing fast ion distributions with $V_{||}/V \sim 0.7-1$ with $D_b = 1 \text{ m}^2/\text{s}$ (right) and without $D_b = 0 \text{ m}^2/\text{s}$ (left) anomalous fast ion diffusion. The tangency point of NBI is highlighted as a cross at $R=0.7\text{m}$, $Z=0\text{m}$.

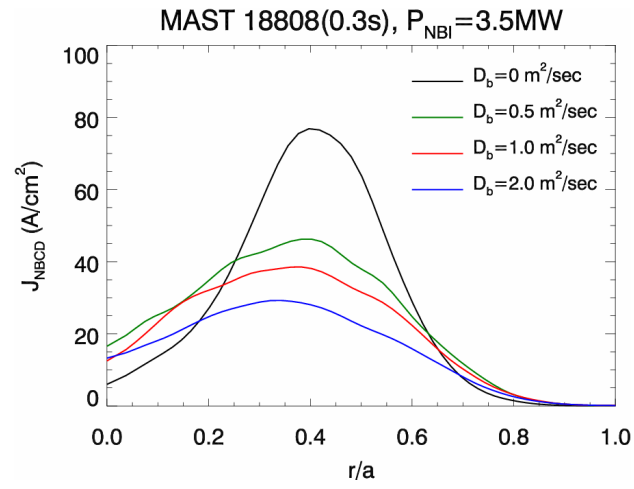


Figure 9. TRANSP simulations of NB driven current density profiles for various values of anomalous fast ion diffusion coefficient, D_b .

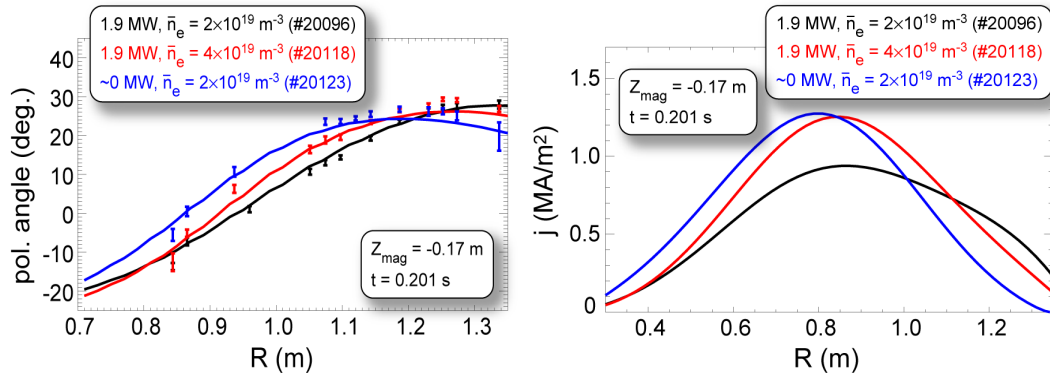


Figure 10. Polarisation angle (left) in off-axis NBI discharges and resulting current density distributions (right) for test set of the MAST discharges with identical plasma current and boundary. Analysis was performed using EFIT95 with simple 1D MSE constraint.